Yuzuncu Yil University
Journal of the Institute of Natural & Applied Sciences

https://dergipark.org.tr/en/pub/yyufbed

Research Article

Physical Properties of Piezoelectric Zr_3GeO_8 Crystal

Mehmet ERZEN

Department of Physics, Institute of Natural and Applied Sciences, Van Yuzuncu Yil University, 65080, Van, Türkiye
Mehmet ERZEN, ORCID No: 0000-0002-7716-8608
Corresponding author e-mail: merzennn@gmail.com

Article Info

Received: 30.11.2022
Accepted: 18.09.2023
Online December 2023

DOI:10.53433/yyufbed.1212067

Keywords
Abinit,
DFT,
Electronic properties,
Optic properties,
Zr_3GeO_8

Abstract: Based on the density functional theory and first-principal calculations, the physical properties of the Zr_3GeO_8 crystal for the ground state were calculated. In all calculations, the Density functional theory based ABINIT package program was used. Investigations were made under the local density approximation. The geometric optimization of the Zr_3GeO_8 crystal, the state density of the valence electrons, the electronic band structure to understand the conductivity character of the crystal, and the linear optical properties to see the response of the material to the electromagnetic wave were calculated. In addition, dynamic-thermodynamic properties were calculated for the Zr_3GeO_8 crystal. According to the calculated structural optimization and electronic band structure, the band gap of the Zr_3GeO_8 crystal is 4.4663 eV and it has been obtained that it has an indirect band gap. For the Zr_3GeO_8 crystal, some constants such as energy loss functions, reflectivity, and absorption coefficient are calculated depending on the ground state linear optical properties and linear optical properties. The phonon distribution, state density and contribution of each atom to the density of state the Zr_3GeO_8 crystal were calculated. Finally, free energy, internal energy, entropy, and heat capacity were calculated for the Zr_3GeO_8 crystal.

Piezoelektrik Zr_3GeO_8 Kristalinin Fiziksel Özellikleri

Makale Bilgileri

Geliş: 30.11.2022
Kabul: 18.09.2023
Online Aralık 2023

DOI:10.53433/yyufbed.1212067

Anahtar Kelimeler
Abinit,
DFT,
Elektronik özellikler,
Optik özellikler,
Zr_3GeO_8

Öz: Yoğunluk fonksiyonel teorisine ve ilk temel hesaplamalara dayanarak, Zr_3GeO_8 kristalinin temel durum için fiziksel özellikleri hesaplanmıştır. Yapılan tüm hesaplamalarda Yoğunluk fonksiyonel teorisi tabanlı çalışan ABINIT paket programı kullanılmıştır. İncelemeler yerel yoğunluk yaklaşımı altında yapılmıştır. Zr_3GeO_8 kristalinin geometrik optimizasyonu, valans elektronlarının durum yoğunluğu, kristalin iletkenlik karakterini anlamak için elektronik bant yapısı, malzemenin elektromanyetik dalgaya tepkisini görmek için doğrusal optik özellikleri hesaplanmıştır. Ayrıca Zr_3GeO_8 kristali için dinamik-termodinamik özellikleri hesaplanmıştır. Hesaplanan yapısal optimizasyon ve elektronik bant yapısına göre Zr_3GeO_8 kristalinin bant aralığı 4.4663 eV olup dolaylı bir bant aralığına sahip olduğu elde edilmiştir. Zr_3GeO_8 kristali için temel durumdaki lineer optik özellikler ve lineer optik özelliklere bağlı olarak enerji kaybı fonksiyonları, yansıtma ve absorpsiyon katsayısı gibi bazı sabitler hesaplanır. Zr_3GeO_8 kristalinin fonon dağılımı, durum yoğunluğu ve her bir atomun durum yoğunluğuna katkısı hesaplandı. Son olarak Zr_3GeO_8 kristali için serbest enerji, iç enerji, entropi ve ısı kapasitesi hesaplanmıştır.

1. Introduction

As it is known, the first proof of the direct piezoelectric effect was made by the brothers Pierre Curie and Jacques Curie in 1880. However, the Curie brothers were not aware of the reverse piezoelectric effect (Curie & Curie, 1880; Dineva et al., 2014). The inverse piezoelectric effect was mathematically demonstrated by Gabriel Lippmann, starting from the fundamental thermodynamic principles. Many more studies were carried out to discover crystal structures exhibiting piezoelectric properties. 20 out of 32-point groups have piezoelectric properties. 10 of them exhibit pyroelectric properties. Zr_3GeO_8 crystal has $\bar{4}2m$ point group. Such crystals are important in the technological field due to their piezoelectric properties. Many studies have not been done for Zr_3GeO_8 crystal in the literature. Lattice parameters and atomic positions were obtained for the conventional structure of the Zr_3GeO_8 crystal by neutron diffraction method (Ennaciri et al., 1984). Nanoparticles consisting of these oxides, zirconia, and germanium were added to Silica sol-gel glasses and Zr-Ge-O binary oxides were produced in matrices. $ZrGeO_4$ and Zr_3GeO_8 nanoparticles in solid matrices were produced for the first time (Gurin et al., 2005). The reaction products of ZrO_2 and GeO_2 powders were characterized by quantitative phase analysis. X-ray diffraction and Raman spectroscopy data showed that the Zr_3GeO_8 and $ZrGeO_4$ almanacs were formed. Moreover, a study was conducted on Zirconium Germanates to demonstrate their Synthesis, Stoichiometry, and Thermal Behaviors (Utkin et al., 2012 and 2013). Finally, theoretical calculations have been made for the Zr_3GeO_8 crystal using the density functional theory and GGA / GGA+U / R2SCAN methods in the literature (Jain et al., 2013).

As can be seen, these properties were not calculated in detail under the local density approximation of the Zr_3GeO_8 crystal. Piezoelectric crystals have an important place in the technological field. The Zr_3GeO_8 crystal was chosen for this study because of its piezoelectric property. In addition, it has been discussed since there is no detailed theoretical study for Zr_3GeO_8 crystal under the LDA approximation in the literature.

2. Material and Methods

The space group of the Zr_3GeO_8 crystal with a total of 12 atoms in its unit cell is I-42m (No.121). The unit cell created by Vesta is given in Figure 1 (Momma & Izumi, 2011). To obtain the physical properties of the Zr_3GeO_8 crystal under density functional theory (DFT), using the ABINIT (Gonze et al., 2002) package program to determine the characteristics of the crystal, the electronic band structure, the state density of the valence electrons of the crystal (DOS), linear optical properties and accordingly Some optical constants have been calculated. In addition, the dynamic and thermodynamic properties of Zr_3GeO_8 crystal were calculated. In this study, Troullier-Martins-type pseudopotentials were produced with FHI (FHI98PP) code by taking into account local density approximation (LDA), and only valence electrons were used (Troullier & Martins, 1991; Fuchs & Scheffler, 1999). Cutoff energy was chosen as 35 Hartree in all calculations. In addition, a Brillouin zone (BZ) 10×10×10 Monkhorst–Pack mesh grid was used (Monkhorst & Pack, 1976).

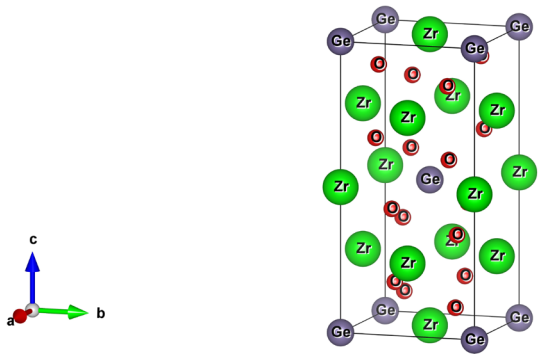

Figure 1. The unit cell of Zr_3GeO_8 crystal.

3. Results

3.1. Structural optimization of the Zr_3GeO_8 crystal

For the unit cell of the Zr_3GeO_8 crystal, structural optimization was first performed under the local density approximation. As a result of the optimization, as seen in Figure 2, the volume value corresponding to the minimum energy was obtained as 839.29 $Bohr^3$. The lattice parameter given in the literature for the unit cell of the Zr_3GeO_8 crystal is 12.11 Bohr (Jain et al., 2013). The lattice parameter we obtained as a result of the calculation we made is 11.73 Bohr.

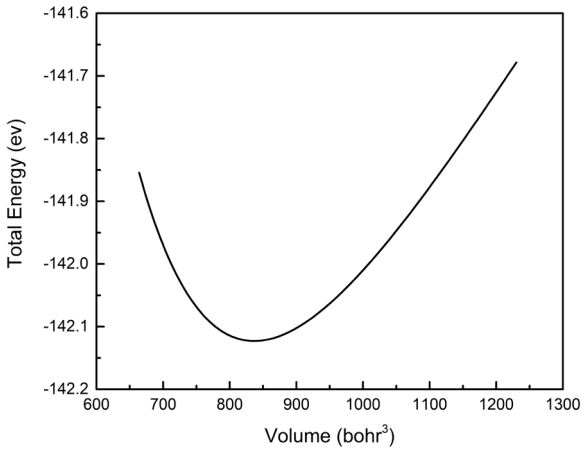

Figure 2. Variation of total energy by volume for a Zr_3GeO_8 crystal.

3.2. Electronic band structure of the Zr_3GeO_8 crystal

Electronic band structure has an important place in terms of the use of materials in the technological field. By using the lattice parameters obtained in the structural optimization of the Zr_3GeO_8 crystal, the band structure of the crystal was calculated along the high symmetry points in the Brillouin region (BZ) to learn the conductivity character of the crystal by considering only the valence electrons of the piezoelectric Zr_3GeO_8 crystal. The total density of the state and electronic band structure in the BZ of the crystal is shown in Figure 3. As a result of the calculation of the band structure of Zr_3GeO_8 for the high symmetry points observed in the BZ, considering the space group to which the crystal belongs, it was obtained that the Γ-X symmetry points in BZ correspond to the top of the valence bands. It was found that the lower part of the conduction bands coincides with the Z and M points, which are the center of the BZ. Therefore, Zr_3GeO_8 is an insulator and as seen in Figure 3, the band transitions correspond to different points and the indirect band gap is 4.4663 eV.

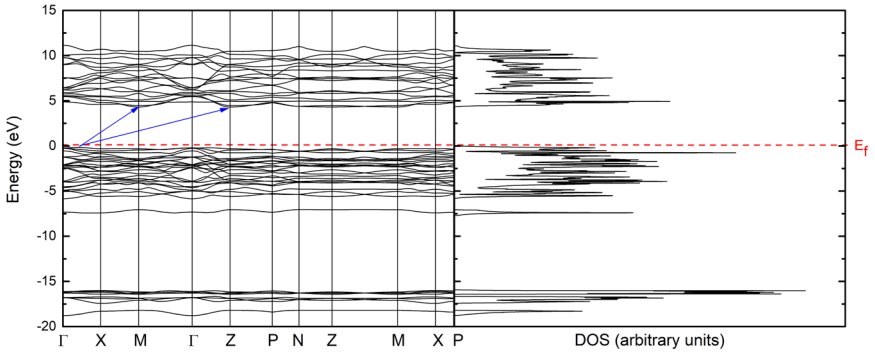

Figure 3. The electronic band structure and total density of state (DOS) for a Zr_3GeO_8 crystal.

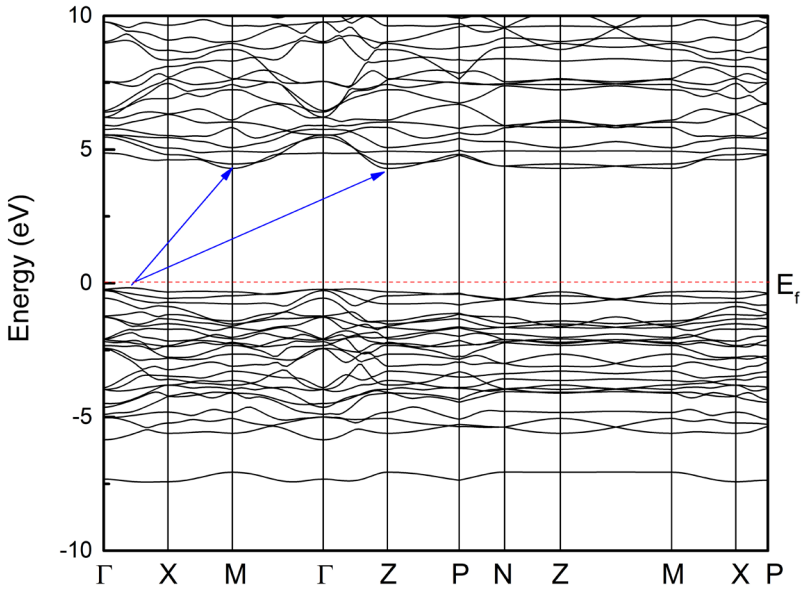

Figure 4. The electronic band structure of Zr_3GeO_8 crystal between -10 eV and 10 eV.

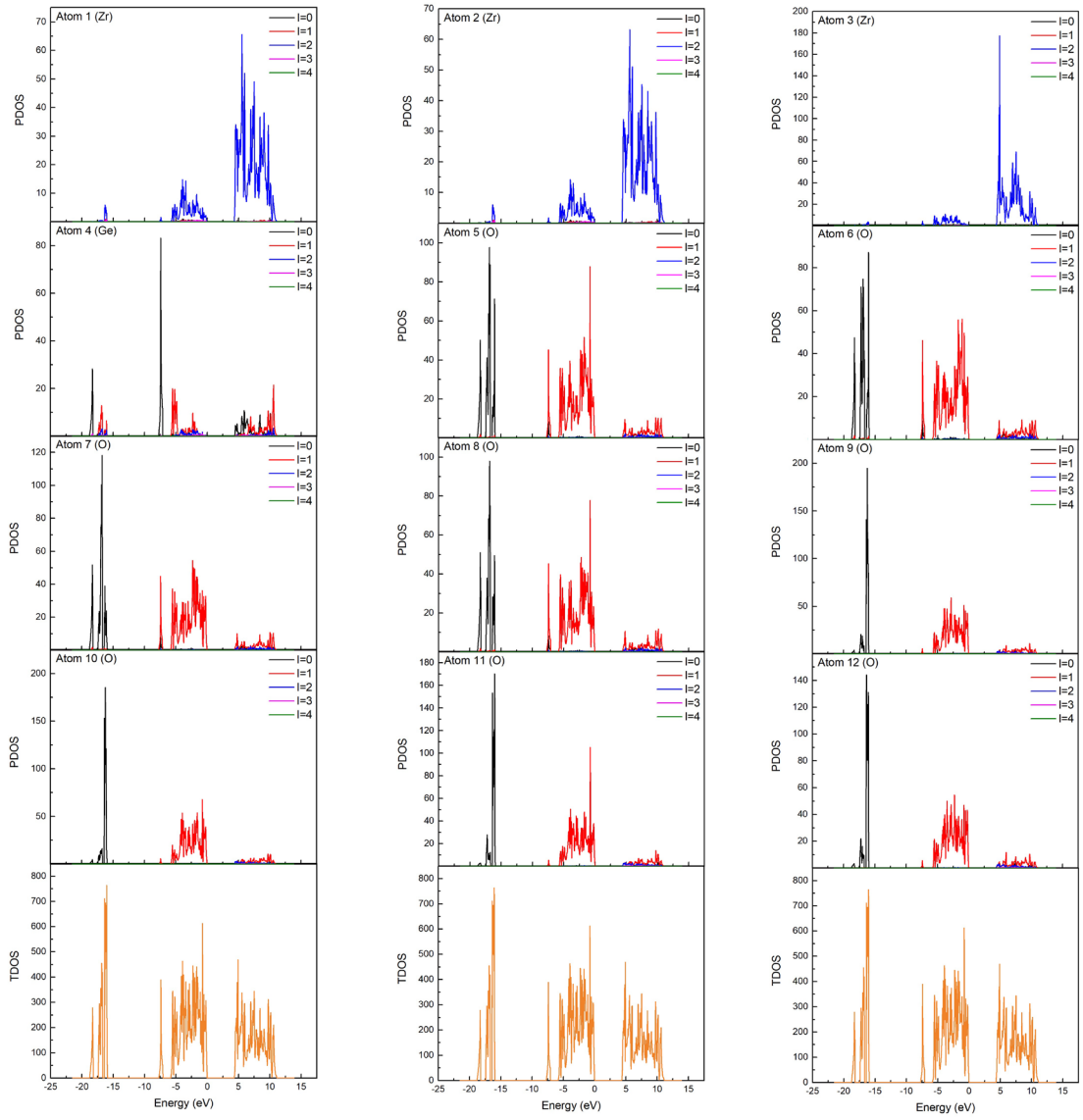

Figure 5. The partial (PDOS) and total (TDOS) DOS's for crystal Zr_3GeO_8.

Then, the contributions of the partial density of state (PDOS) to the total density of state (TDOS) of the whole crystal were calculated for the Zr, Ge, and O atoms forming the Zr_3GeO_8 crystal. All calculated density of state (PDOS-TDOS) is shown in Figure 5. Here, the oxygen atoms make the most contribution to the total DOS for the l=0 and l=1 levels. Similarly, for the l=2 level, the most contribution is made by the zirconium atoms. Here l=0 level to s orbital, l=1 level to p orbital, etc. corresponds. Therefore, when we look at the electronic configurations of the elements, it is expected that the O atom will contribute the most to the l=0 level. Also, the number of identical atoms in the unit cell affects the contribution.

3.3. Optical properties of the Zr_3GeO_8 crystal

The optical properties of semiconductors, which are especially important in the electronics industry, are quite wide. It is well known that the optical properties of a material are obtained with the dielectric tensor, which has imaginary and real parts, considering the frequency of the electromagnetic wave incident on the material. Furthermore, both the real and imaginary parts of the complex dielectric function are linked by Kramers-Kronig relations (Erzen & Akkus, 2018). The real and imaginary parts of the dielectric function for the Zr_3GeO_8 crystal were calculated under the local density approximation. The results obtained are shown in Figure 6. If the actual portion of the dielectric components of a crystal enters the negative region, the crystal in the negative region exhibits optically metallic properties. Figure 6 shows that the Zr_3GeO_8 crystal enters the negative range of about 14 eV to 27 eV in all directions. The static dielectric constant of the Zr3GeO8 crystal in all directions ($\varepsilon_0^{11}, \varepsilon_0^{22}, \varepsilon_0^{33}$) was calculated. These are 3.1983 in direction 11, 3.2866 in direction 22, and 3.3565 in direction 33. ε_2 represents the imaginary part of the dielectric function and the energy losses. Looking at the ε_2 graph, it is seen that it is stable from 0 to about 4 eV. This corresponds to the band gap of the material.

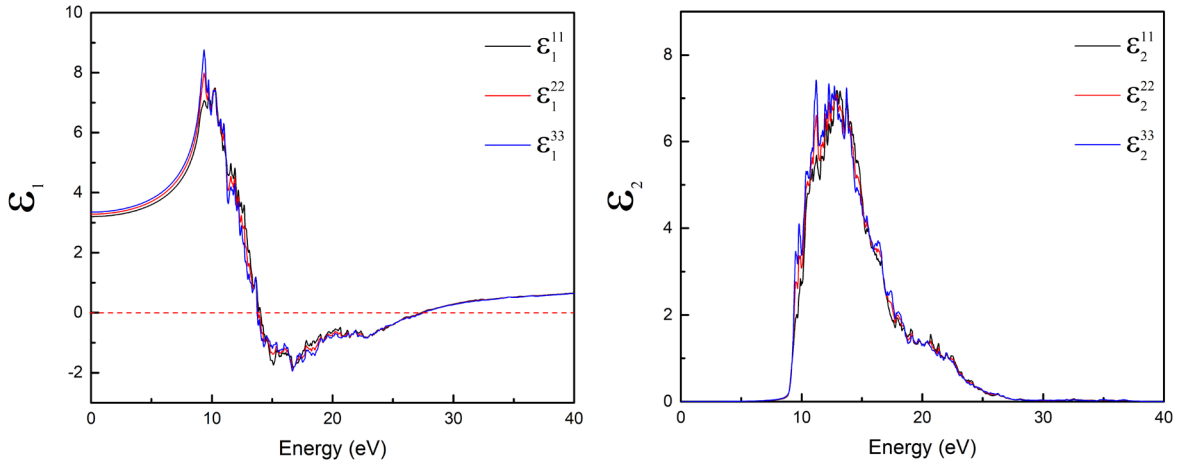

Figure 6. Variation of Zr_3GeO_8 versus photon energy of ε_1 and ε_2 in different crystal axes.

The refractive index of the Zr_3GeO_8 crystal with respect to axes (n_{11}, n_{22}, n_{33}) and the variation of the refractive index of the light against the wavelength was calculated as in Figure 7. The obtained refractive index values are 1.7905 in the 11 direction, 1.8116 in the 22 direction, and 1.8309 in the 33 direction. In addition, some optical constants such as energy loss functions, extinction coefficient, reflectivity, and absorption coefficient are calculated using the real and imaginary parts of the dielectric function and are given in Figure 8.

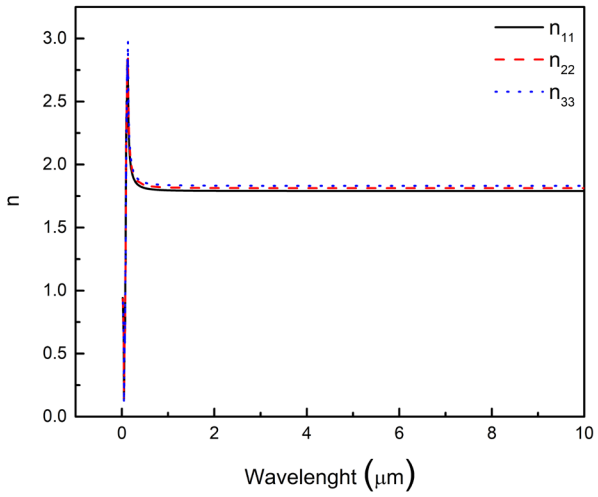

Figure 7. Variation of the refractive index of Zr_3GeO_8 crystal with respect to axes against wavelength.

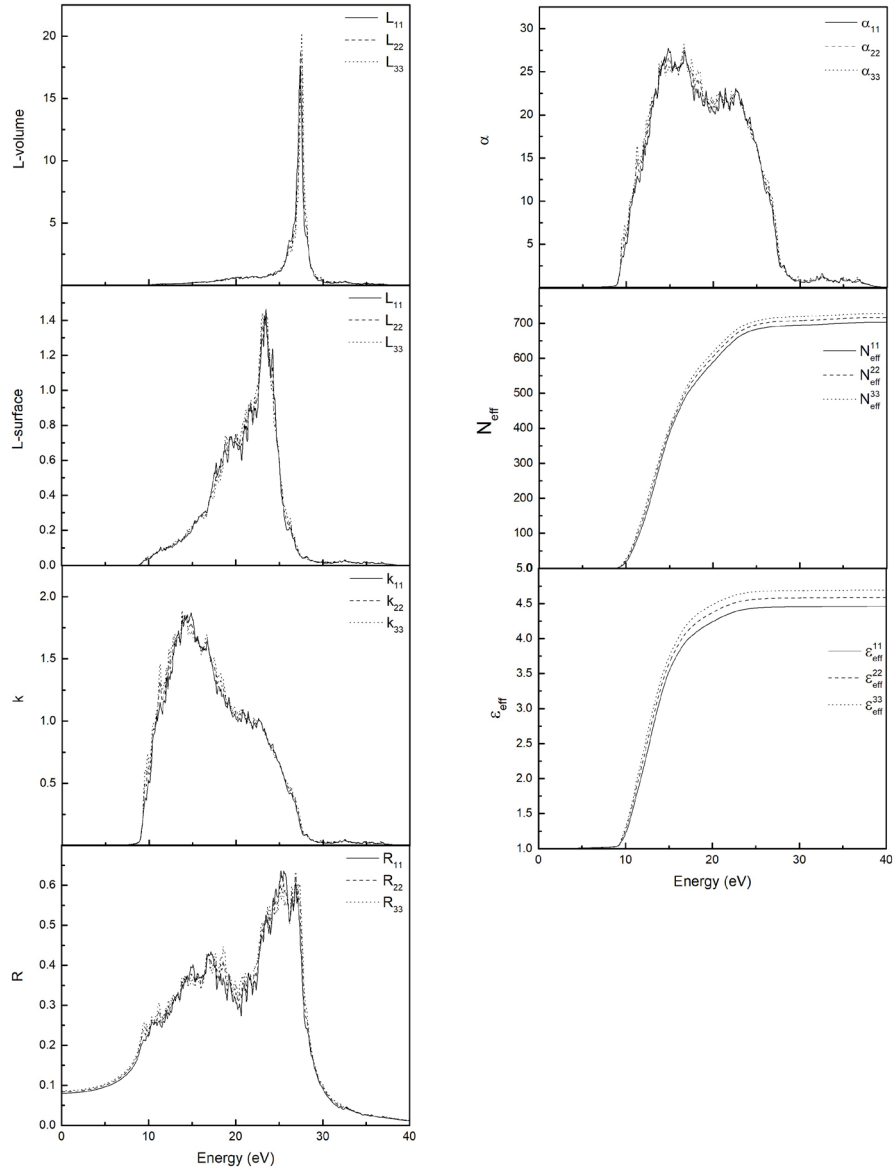

Figure 8. Optical constants of Zr_3GeO_8 in the direction of different crystal axes; Energy loss functions (L), absorption coefficient (α), extinction coefficient (k), reflectivity (R), effective dielectric constant (ε_{eff}), and effective valence electron number (N_{eff}).

3.4. Dynamic and thermodynamic properties of the Zr_3GeO_8 crystal

The vibrational properties of phonons have an important place in crystal structures. In this study, the phonon distribution of the Zr_3GeO_8 crystal was obtained. The phonon distribution of the Zr_3GeO_8 crystal was obtained by using the 4×4×4 Monkhorst-Pack mesh grid for the ground state. The phonon distribution and phonon state density (PHDOS) for the Zr_3GeO_8 crystal were calculated as shown in Figure 9. There are a total of 36 modes for the Zr_3GeO_8 crystal with 12 atoms. As seen in Figure 9, the modes do not enter the negative region. This indicates that the crystal is dynamically stable. In addition, as shown in Figure 10, the total PHDOS of Zr_3GeO_8 and the contribution of Zr, Ge, and O atoms separately to PHDOS were obtained. The phonon density of states tells us how many phonon modes are present at each frequency.

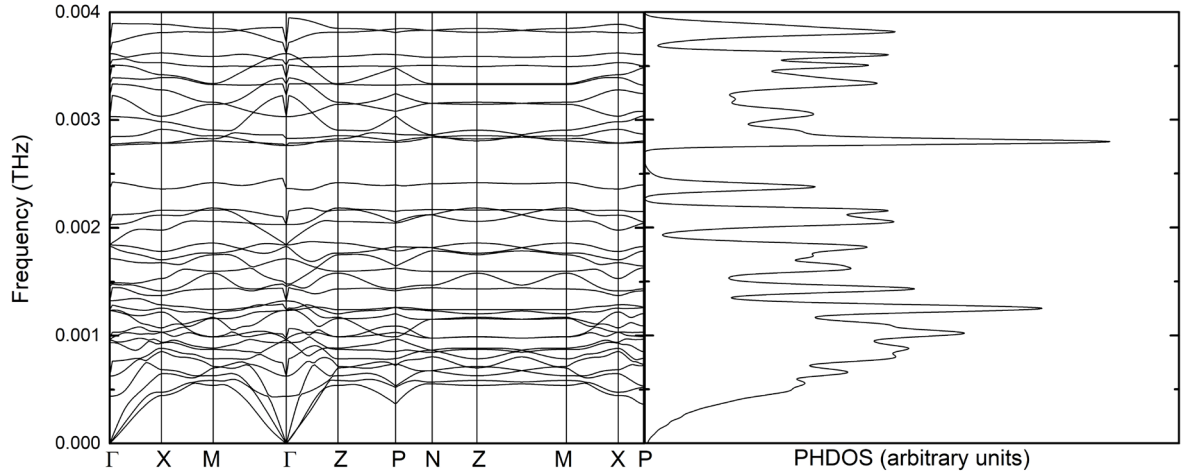

Figure 9. The phonon distribution for the Zr_3GeO_8 crystal and the corresponding phonon density of states.

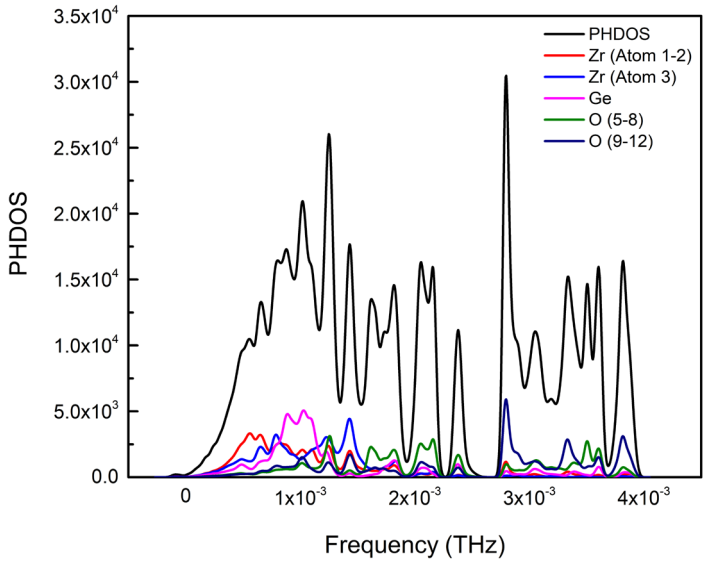

Figure 10. Contributions of each atom to PHDOS for the Zr_3GeO_8 crystal.

Internal energy refers to the sum of the energies of interactions such as the kinetic energy resulting from the movements of its particles in a system and the force that holds physical or chemical bonds together. It is defined as the derivative of heat capacity and the heat of an object with respect to its temperature. Free energy is a concept related to the conversion of the energy potential of a chemical reaction into work. In thermodynamics, entropy is the concept that represents the thermal energy of a

system that cannot be converted into mechanical work. As seen in Figure 11., the variation of internal energy (E), heat capacity (C), free energy (F), and entropy (S) with temperature was calculated for the Zr_3GeO_8 crystal using the phonon distribution of the Zr_3GeO_8 crystal and the phonon density of the states. Also the contribution of phonons to internal energy and free energy at absolute temperature is approximately 9.2×10^4 J mol^{-1} and 9.19×10^4 J mol^{-1}, respectively.

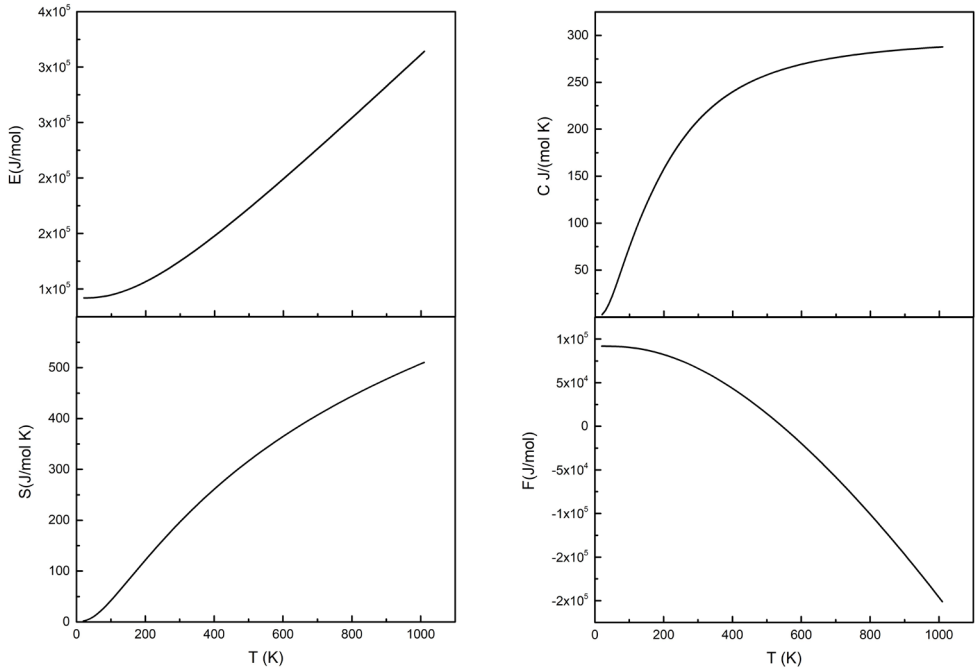

Figure 11. Variation of E, F, S, and C of Zr_3GeO_8 depending on temperature.

4. Discussion and Conclusion

In this theoretical study, the physical properties of the piezoelectric Zr_3GeO_8 crystal were calculated with the density functional theory. First, structural optimization calculation was performed to obtain the stable state of the Zr_3GeO_8 crystal. Then, using the data obtained in structural optimization, the electronic band structure of Zr_3GeO_8 along the path determined in BZ was calculated and the indirect band gap of Zr_3GeO_8 was obtained as 4.4663 eV. In addition, DOS calculation was performed to determine the number of enterable states corresponding to the unit frequency range of the valence electrons of the Zr_3GeO_8 crystal. In the literature, the band gap for the Zr_3GeO_8 crystal was obtained as 3.9 eV by using the GGA / GGA+U / R2SCAN methods. In this study, the band gap was calculated as 4.4663 eV using the local density approximation. The reason why the calculated band gap differs from the value in the literature is the approximations used. In order to determine the response of the Zr_3GeO_8 crystal to the electromagnetic wave on it, linear optical properties and some optical constants were investigated. Finally, the dynamic-thermodynamic properties of piezoelectric Zr_3GeO_8 are discussed as a result of the calculations. In the calculations made, it was determined that the Zr_3GeO_8 crystal was dynamically stable. In addition, the change of some thermodynamic potentials of Zr_3GeO_8 crystal against temperature was investigated thermodynamically. It was observed that entropy, internal energy, and heat capacity increased as expected with increasing temperature. For Zr_3GeO_8 crystal, no comparison has been made since there is no study in the literature as dynamics-thermodynamics under the local density approximation.

In the literature review, there is no detailed theoretical study for Zr_3GeO_8 crystal under the local density approximation. Therefore, no comparison has been made. This study will be helpful for future studies.

References

Curie, J., & Curie, P. (1880). Développement par compression de l'électricité polaire dans les cristaux hémièdres à faces inclinées. *Bulletin de Minéralogie*, 3(4), 90-93. doi:10.3406/bulmi.1880

Dineva, P., Gross, D., Müller, R., & Rangelov, T. (2014). Piezoelectric materials. *In Dynamic Fracture of Piezoelectric Materials* (pp. 7-32). Springer, Cham. doi:10.1007/978-3-319-03961-9_2

Ennaciri, A., Michel, D., y Jorba, M. P., & Pannetier, J. (1984). Neutron diffraction determination of the structure of an ordered scheelite-type: Zr_3GeO_8. *Materials Research Bulletin*, 19(6), 793-799. doi:10.1016/0025-5408(84)90037-0

Erzen, M., & Akkus, H. (2018). Effect of pressure on physical properties of $LuAsO_4$ crystal. *Materials Research Express*, 5(11), 116204. doi:10.1088/2053-1591/aade2c

Fuchs, M., & Scheffler, M. (1999). Ab initio pseudopotentials for electronic structure calculations of poly-atomic systems using density-functional theory. *Computer Physics Communications*, 119(1), 67-98. doi:10.1016/S0010-4655(98)00201-X

Gurin, V. S., Alexeenko, A. A., Kasparov, K. N., & Tyavlovskaya, E. A. (2005). Incorporation of zirconia and germania and ternary compounds of ZrO_2–GeO_2 into silica sol-gel matrices. *Materials Science-Poland*, 23(1), 49-60.

Gonze, X., Beuken, J. M., Caracas, R., Detraux, F., Fuchs, M., Rignanese, G. M., … & Allan, D. C. (2002). First-principles computation of material properties: the ABINIT software project. *Computational Materials Science*, 25(3), 478-492. doi:10.1016/S0927-0256(02)00325-7

Jain, A., Ong, S. P., Hautier, G., Chen, W., Richards, W. D., Dacek, S., … & Persson, K. A. (2013). The Materials Project: A materials genome approach to accelerating materials innovation. *APL Materials*, 1(1), 011002. doi:10.1063/1.4812323

Momma, K., & Izumi, F. (2011). VESTA 3 for three-dimensional visualization of crystal, volumetric and morphology data. *Journal of Applied Crystallography*, 44(6), 1272-1276. doi:10.1107/S0021889811038970

Monkhorst, H. J., & Pack, J. D. (1976). Special points for Brillouin-zone integrations. *Physical Review B*, 13(12), 5188. doi:10.1103/PhysRevB.13.5188

Troullier, N., & Martins, J. L. (1991). Efficient pseudopotentials for plane-wave calculations. *Physical Review B*, 43(3), 1993. doi:10.1103/PhysRevB.43.1993

Utkin, A. V., Bulina, N. V., Belen'kaya, I. V., & Baklanova, N. I. (2012). Phase analysis of the ZrO_2-GeO_2 system. *Inorganic Materials*, 48(6), 601-606. doi:10.1134/S0020168512060209

Utkin, A., Baklanova, N., & Vasilieva, I. (2013). *Zirconium germanates: Synthesis, stoichiometry and thermal behavior.* 14th European Conference on Solid State Chemistry, Bordeaux, France. doi:10.13140/2.1.4851.7444.